Published in final edited form as:
Free Radic Biol Med. 2013 March ; 56: 17–27. doi:10.1016/j.freeradbiomed.2012.11.018.

Manganese superoxide dismutase depletion in murine hematopoietic stem cells perturbs iron homeostasis, globin switching, and epigenetic control in erythrocyte precursor cells

Adam J. Case[1], **Joshua M. Madsen**[1], **David G. Motto**[2], **David K. Meyerholz**[3], and **Frederick E. Domann**[1,*]

[1]Free Radical and Radiation Biology Program, Department of Radiation Oncology, Holden Comprehensive Cancer Center, The University of Iowa, Iowa City, IA 52242, USA

[2]Division of Hematology Oncology, Department of Internal Medicine, The University of Iowa, Iowa City, IA 52242, USA

[3] Department of Pathology, The University of Iowa, Iowa City, IA 52242, USA

Abstract

Heme synthesis partially occurs in the mitochondrial matrix, thus there is a high probability that enzymes and intermediates important in the production of heme will be exposed to metabolic byproducts including reactive oxygen species. In addition, the need for ferrous iron for heme production, Fe-S coordination, and other processes occurring in the mitochondrial matrix suggests that aberrant fluxes of reactive oxygen species in this compartment might perturb normal iron homeostasis. Manganese superoxide dismutase (*Sod2*) is an anti-oxidant enzyme that governs steady-state levels of the superoxide in the mitochondrial matrix. Using hematopoietic stem cell-specific conditional *Sod2* knock-out mice we observed increased superoxide concentrations in red cell progeny which caused significant pathologies including impaired erythrocytes and decreased ferrochelatase activity. Animals lacking *Sod2* expression in erythroid precursors also displayed extramedullary hematopoiesis and systemic iron redistribution. Additionally, the increase in superoxide flux in erythroid precursors caused abnormal gene regulation of hematopoietic transcription factors, globins, and iron-response genes. Moreover, the erythroid precursors also displayed evidence of global changes of histone post-translational modifications, a likely cause of at least some of the aberrant gene expression noted. From a therapeutic translational perspective, mitochondrially-targeted superoxide-scavenging anti-oxidants partially rescued the observed phenotype. Taken together, our findings illuminate the superoxide sensitivity of normal iron homeostasis in erythrocyte precursors and suggest a probable link between mitochondrial redox metabolism and epigenetic control of nuclear gene regulation during mammalian erythropoiesis.

* To whom correspondence should be addressed: **Frederick E. Domann**, Free Radical and Radiation Biology Program, The Department of Radiation Oncology, Carver College of Medicine, The University of Iowa, B180 Medical Laboratories, Iowa City, IA, USA, Tel: (319) 335-8019; Fax: (319) 335-8039; frederick-domann@uiowa.edu.

COMPETING INTEREST
The authors declare no financial, personal, or professional competing interest in regards to this work.

Keywords

Manganese Superoxide Dismutase; Cre/loxP; Transgenic; Mouse; Ferrochelatase; Anemia; Extramedullary Hematopoiesis; Mitochondria; Anti-Oxidants; N-Acetyl Cysteine; Mito-Tempol

INTRODUCTION

The mitochondrion is the center of eukaryotic cellular metabolism, respiration, and numerous other cellular processes. The byproducts of some of these processes are reactive oxygen species (ROS) and free radicals, which have the ability to directly damage cellular components, change the redox balance of a cell, as well as alter gene regulation through redox sensitive transcription factors [1-4]. Superoxide free radicals ($O_2^{\bullet -}$) produced in the mitochondrial matrix are neutralized by a specific mitochondrial isoform of the superoxide dismutase family known as manganese superoxide dismutase (*Sod2*). Loss or down-regulation of this enzyme has proven to be detrimental to cellular, as well as organismal, viability [5-7]. Due to the well documented role of free radicals and iron, it is presumed that *Sod2* plays a definitive role in maintaining the proper redox balance necessary for normal heme synthesis; a cellular process that partially occurs within the mitochondrion [8].

Ferrous iron (Fe^{2+}) and ferric iron (Fe^{3+}) have been known to play a role in ROS production since the late 1800's [9, 10]. The ability of iron to cycle between oxidation states creates the potential for excess ROS production if iron is not tightly regulated. Iron mobilization and sequestering enzymes such as transferrin or ferritin, respectively, bind iron rendering it relatively inert compared to labile iron [11]. A small unbound labile iron pool is present in the cytoplasm of cells, and functions as the transient iron collection produced from both anabolic and catabolic cellular processes [12]. Oxidative stress has been shown to cause the oxidation of certain iron-sulfur cluster enzymes, which releases iron into the labile iron pool [13, 14]. Moreover, many of these iron-sulfur containing enzymes are located in the mitochondrial matrix, which subjects them to potential shifts in pH and redox balances. Normally, *Sod2* acts to minimize an oxidizing environment in the mitochondria, but how mitochondrial processes (iron dependent and independent) function in the absence of this enzyme remains uninvestigated.

Ferrochelatase (FECH) is the last enzyme in heme biosynthesis, and catalyzes iron insertion into protoporphyrin IX to form heme within the mitochondrial matrix [15]. FECH functions as a dimer, and possesses a single 2-iron, 2-sulfur (2Fe/2S) cluster per monomer [16]. While the 2Fe/2S cluster within the enzyme does not participate in catalysis, if iron is depleted or not bioavailable the apo-enzyme lacking a cluster becomes unstable and this significantly decreases FECH activity [17]. Furthermore, unlike the majority of known 2Fe/2S cluster enzymes (*e.g.* cytochromes, ferredoxins, etc.), FECH possesses an unusual cysteine coordinating motif with limited hydrogen bonding to the iron and sulfur moieties [18]. This partial bonding has been shown to render FECH susceptible to inactivation by free radical species such as nitric oxide ($NO^{\bullet}$) [19, 20]. While mitochondrially located $NO^{\bullet}$ may play a role in the inactivation of FECH, mitochondrially located $O_2^{\bullet -}$ may also have a significant impact during times of pathogenesis. It has been estimated that approximately 2×10^{10} superoxide anions are produced each day within the mitochondria, but under normal physiologic conditions *Sod2* keeps steady state levels of superoxide to in the low pico-molar range [21, 22]. In contrast, during times of pathogenesis or lack of *Sod2* the steady state levels may be increased 5-10 fold [5, 23, 24]. Combining the knowledge of this concentration differential with the understanding that $O_2^{\bullet -}$ is a potent disruptor of certain other Fe/S cluster containing enzymes [14, 25], we hypothesized that increased steady-state levels of mitochondrial superoxide may have the ability to perturb iron homeostasis and

therefore directly or indirectly inactivate FECH. Furthermore, due to evidence demonstrating that the inactivation of mitochondrial metabolic enzymes (*e.g.* aconitase, succinate dehydrogenase, isocitrate dehydrogenase, etc.) may affect gene expression through a loss of epigenetic control [26, 27], we would also expect increased mitochondrial superoxide to affect global cellular gene regulation.

To test these hypotheses, we used a conditional knock-out mouse of the mitochondrial matrix enzyme manganese superoxide dismutase (*Sod2*) with deletion targeted to hematopoietic stem cells. Our results demonstrate that the conditional loss of *Sod2* in the hematopoietic system leads to a severe anemia and redistribution of systemic iron pools due at least in part to inactivation of FECH. Furthermore, there was an apparent loss of regulation of erythropoietic transcription factors, fetal/adult globins, as well as iron response element (IRE) containing genes that was associated with and partially due to global epigenetic changes in hematopoietic precursor cells. Finally, we show that anti-oxidants targeted to the mitochondria have the ability to partially rescue the observed phenotype in our mouse model. Taken together, our findings provide evidence for a previously undescribed consequence for increased mitochondrial $O_2^{\bullet -}$ or *Sod2* inactivation in iron regulation of erythropoietic precursors.

MATERIALS AND METHODS

Mice

Mice homozygous for the floxed *Sod2* allele (*i.e.* B6.Cg-*Sod2*^{tm1lox}, shorthand *Sod2*$^{L/L}$), in which exon 3 of the *Sod2* gene is flanked by 2 loxP sequences, have been previous described [28]. B6.Cg-Tg-v*av1-iCre*^{A2Kio}/J or vav-iCre mice (Cre recombinase is exogenously expressed under control of the vav promoter, where Cre-recombinase becomes activated within the hematopoietic stem cell and affects all lymphoid, myeloid, and erythroid lineages) were generously donated by Dr. Adam Dupuy (The University of Iowa), and have been previously described [29]. Mice were bred to F2 generation to obtain conditional hematopoietic *Sod2* homozygous knock-out animals (*i.e.* *Sod2*$^{-/-}$). Vav-iCre was only passed through male parents to limit non-specific oocyte expression. Mice used were of pure C57BL/6 background, and littermate floxed animals (*i.e.* *Sod2*$^{L/L}$) served as controls. All work was performed under the approval of the Institutional Animal Care and Use Committee at The University of Iowa.

Characterization and Oxidative Stress

Genotyping, real-time quantitative RT-PCR, western blotting, dihydroethidium (DHE) assays, and aconitase activity assays were performed as previously described [5]. For DHE analysis and aconitase activity, respective tissues were minced to single cell suspensions and total cell preparations were analyzed. Oligonucleotide sequences are referenced at the end of the Supplementary Data. Histones were isolated by using acid extraction. Briefly, cells are lysed in histone extraction buffer (*i.e.* PBS with 0.5% Triton-X100, 2 mM phenylmethylsufonyl fluoride, and 0.02% NaN_3). Following lysis, samples are centrifuged at 5,000 RCF at 4°C. Pellets are resuspended in 0.2N HCl overnight. Samples are then centrifuged again at 5,000 RCF at 4°C, and supernatants are collected for analysis. For all experiments, fresh tissue was harvested and used from equal numbers of male and female animals at 6-8 weeks of age, unless otherwise noted. Peripheral blood was isolated by retro-orbital bleeding into heparin coated capillary tubes. Bone marrow was obtained by performing and combining bilateral femur flushes. Solid organs (*e.g.* spleen and thymus) were dissociated by physical disruption using ground glass. Following this, mononuclear cells were isolated by mouse optimized FicoLite-LM gradient (Atlanta Biologicals, Atlanta, GA).

Complete Blood Count (CBC), Iron Panel, and TBARS

Freshly isolated blood was diluted 1:10 into 5% BSA diluted in PBS. CBC analysis was performed on an Advia 120 automated hematology analyzer (Bayer Diagnostics) with an algorithm specific for C57BL/6 mice. Plasma iron panels were performed on freshly isolated plasma by the University of Iowa Hospital and Clinics pathology laboratories. Thiobarbituric acid reactive substances (TBARS) assay was performed using the TBARS Assay Kit (Cayman Chemical, Ann Arbor, MI) as per manufacturer's specifications.

Histology

Tissues were fixed in 10% neutral formalin, then processed and embedded in paraffin. Four- to five-micrometer sections were prepared with a microtome (HM 355, Microm, Walldorf, Germany) and then stained with hematoxylin and eosin (H&E) or Prussian Blue with an automated slide stainer (Sakura DRS 601 Diversified Stainer, Sakura, Hayward, CA). Stained slides were mounted with Solvent 100 mounting media, and bright-field micrographs of stained sections were taken with a microscope (Olympus BX-51, Olympus, Melville, NY) fitted with an Olympus DP70 camera (Olympus).

Free Macrocycles and Ferrochelatase

Free macrocycle assays were performed as previously described [30]. Briefly, equal volume or mass of tissue were combined with Celite (Sigma Aldrich, St. Louis, MO) to remove particulate matter. Macrocycles were extracted from the tissue using a 4:1 mixture of ethyl acetate and acetic acid respectively. Hydrochloric acid (1.5 M) was used for final purification of macrocycles. Relative macrocycle levels were measured by fluorescence (excitation 405 nm, emission 609 nm) using a Tecan Infinite M200 96-well plate spectrophotometer. Ferrochelatase activity assays were performed as previously described [17]. Briefly, proteins were isolated and quantified from bone marrow samples. Four-hundred micrograms of bone marrow protein was combined in an assay buffer (20 mM Tris-HCl (pH 8.0), 1% Triton X-100, 1 mM lauric acid) along with 50 μM deuteroporphyrin IX and 50 μM Zn (II) acetate at 37°C. Appearance of zinc loaded porphyrin was observed over time in a Beckman-Coulter DU-650 spectrophotometer at 541 nm absorbance.

Rescue

Hemin was obtained from Sigma Aldrich Company (St. Louis, MO). N-acetyl cysteine (NAC) was obtained from The University of Iowa Pharmacies (20% solution in normal saline, 200 mg/mL). Mito-tempol was obtained from Enzo Life Sciences (Plymouth Meeting, PA). All lyophilized drugs were dissolved in PBS and administered by intraperitoneal (IP) injection. Specific concentrations were chosen based on published therapeutic effects in mice at respective doses. Hemin was administered every 48 hours at 50 mg/kg [31, 32]; NAC administered every 24 hours at 1 g/kg [33, 34]; Mito-tempol administered every 24 hours at 5 mg/kg [5, 35]. Complete blood count analyses were performed at 0, 3, and 7 days while mice were on drug treatment.

Statistics

Data were as expressed as mean and standard deviation. All experiments were performed on at least 3 mice in each group. For all experiments, comparisons between groups were analyzed by unpaired 2-tailed Student's t-test. A p-value of less than 0.01 was considered to be significant.

RESULTS

Steady-state superoxide concentrations increase in conditional Sod2 knock-out tissues

To examine the effects of increased mitochondrial superoxide on erythrocyte development and function, we developed a hematopoietic-specific *Sod2* knock-out mouse (*i.e.* $Sod2^{-/-}$). Mice harboring loxP elements flanking the active site of the *Sod2* locus (*i.e.* $Sod2^{L/L}$) were bred with mice expressing cre-recombinase under the vav promoter, which targets hematopoietic stem cells within the bone marrow [29]. Analysis of the major hematopoietic organs (*e.g.* bone marrow, spleen, and thymus) showed significant knock-out of *Sod2* as demonstrated by decreased immunoreactivity by western blotting (Fig. 1A). Importantly, off target tissues (*i.e.* liver, heart, skin, and brain) did not show any decrease in *Sod2* mRNA (supplemental Fig. 1A) indicating the specificity of the vav promoter for the hematopoietic system, as has been described by others [29, 36, 37].

Sod2 functions to decrease mitochondrial superoxide levels, and as such the loss of the superoxide scavenging enzyme should lead to increased steady-state levels of superoxide. Using the fluorescent dye dihydroethidium (DHE), it was observed that all major hematopoietic organs within $Sod2^{-/-}$ mice showed greater than 3-fold increases in oxidative stress (Fig. 1B, supplemental Fig. 1C). Furthermore, using excitation wavelengths for the superoxide-specific fraction indicated that the increases in fluorescence were primarily due to an increase in superoxide as opposed to other ROS [38]. To extend these findings and determine the biological sequelae of elevated steady-state superoxide in erythroid precursor cells, aconitase activity assays were performed on lysates generated from $Sod2^{-/-}$ hematopoietic organs, since this 4Fe/4S enzyme is known to be inactivated by superoxide [14, 39]. Aconitase enzyme activities were decreased by as much as 75% in the hematopoietic organs examined, with no change in aconitase protein levels, consistent with enzyme inactivation by excess superoxide (Fig. 1C, supplemental Fig. 1B). Although both DHE and aconitase have been shown to react with reactive nitrogen species (RNS) such as peroxynitrite [40], the specific nitration product 3-nitrotyrosine was not detected by western blot in cellular proteins isolated from the hematopoietic organs in either $Sod2^{L/L}$ or $Sod2^{-/-}$ mice (data not shown). Peroxynitrite and nitric oxide still may play a role in the $Sod2^{-/-}$ hematopoietic cells, but are dwarfed by the over-abundance of superoxide and thus are below our current limit of detection. Taken together, these data indicate that $Sod2^{-/-}$ mice harbor increased steady-state levels of mitochondrial superoxide, thus providing an optimal model for studying the consequences of this stress on the development of erythrocytes *in vivo*.

Elevated mitochondrial superoxide in erythroid precursor cells has detrimental effects on mature erythrocytes

Mature red blood cells do not contain *Sod2* protein as they do not possess mitochondria. In contrast, immature erythrocyte precursors rely on mitochondria for oxidative metabolism as well as heme synthesis through the orthochromatic normoblast stage of erythrocyte maturation, thus allowing significant developmental time in which the loss of *Sod2* may exert its effects. Analysis of peripheral blood smears from $Sod2^{-/-}$ mice showed profound differences compared to their $Sod2^{L/L}$ counterparts. The $Sod2^{-/-}$ mice displayed a variety of hematological differences including anisocytosis (no predisposition to macrocytic or microcytic anemia), spherocytosis, and hypochromasia (Fig. 2A).

Quantitative examination of the observed erythrocyte changes by complete blood count (CBC) analysis demonstrated considerable aberrations in the blood of $Sod2^{-/-}$ mice (Fig. 2B). Total red blood cells were shown to be decreased by approximately 30%, while hemoglobin levels and hematocrits were decreased by approximately 50% and 30%

respectively, in the *Sod2*$^{-/-}$ mice. Circulating reticulocyte numbers showed the greatest change in the knock-outs with an almost 10-fold increase, suggesting accelerated erythropoiesis occurring within the *Sod2*$^{-/-}$ mice. These findings demonstrate unequivocally that loss of the mitochondrial enzyme *Sod2* has significant detrimental effects on red blood cell development.

Due to the 10-fold increase of circulating reticulocytes in the *Sod2*$^{-/-}$ mice, we hypothesized that improper erythrocyte development/breakdown and/or systemic hypoxia was resulting in compensatory erythropoiesis. The spleens of control and knock-out animals were examined for histologic signs of pathology as well as extramedullary hematopoiesis (EMH). Grossly, spleens within the *Sod2*$^{-/-}$ animals were approximately 3-4 times greater in size and weight compared to *Sod2*$^{L/L}$ animals. Upon microscopic examination, loss of normal splenic architecture was noted primarily due to an extensive expansion of the red pulp (supplemental Fig. 2A). Furthermore, detailed analysis of the red pulp displayed elements of all hematopoietic lineages (*e.g.* neutrophils, megakaryocytes, lymphocytes, and erythrocytes) suggesting the spleen is functioning in excess of *Sod2*$^{L/L}$ controls (supplemental Fig. 2B). These changes are consistent with an approximate 25-fold induction of erythropoietin (EPO) mRNA observed within the kidneys of *Sod2*$^{-/-}$ animals (supplemental Fig. 2C). The expansive erythropoiesis was not limited only to the spleen, as blood forming elements were observed to a lesser extent in the livers of the *Sod2*$^{-/-}$ animals as well (supplemental Fig. 3A). *Sod2*$^{-/-}$ mouse livers did not show significant morphologic changes from *Sod2*$^{L/L}$ except for increased incidence of EMH. Alanine aminotransferase (ALT, supplemental Fig. 3B) was similar between *Sod2*$^{L/L}$ and *Sod2*$^{-/-}$, which would further indicate a lack of hepatocellular damage; however, the concurrent elevation in aspartate aminotransferase (AST) strongly suggests an extra-hepatic tissue source, the most prominent candidate tissue in this case would likely be damaged erythrocytes (which also possess AST activity).

Iron homeostasis and distribution are disrupted within Sod2$^{-/-}$ mice

Superoxide has the ability to affect iron metabolism due to its ability to alter iron oxidation states in a variety of systems. Prussian blue analysis of *Sod2*$^{-/-}$ spleens demonstrated strong positive staining for iron, but spatial distribution of the iron varied significantly compared to spleens from *Sod2*$^{L/L}$ animals (Fig. 3). Whereas control spleens showed uniform iron staining contained within areas of the red pulp, the knock-out spleens displayed heterogeneous deposits of iron throughout the entire spleen including white pulp regions. These findings are most likely attributed to the increased EMH and oxidative stress also noted within these tissues of the knock-out animals. Another possible explanation for the aberrant iron distribution could be a failure of the marginal zone macrophages, which are phagocytic cells that interact with apoptotic debris at the boundary of the red and white pulp in the spleen. These marginal zone macrophages would also be devoid of *Sod2* in the knock-out animals due to gene recombination early in hematopoietic development, and as such may malfunction in their role of appropriately maintaining iron recycling and distribution in the spleen. The disruption in iron homeostasis within the spleens of *Sod2*$^{-/-}$ animals was not a specific organ effect, as a systemic redistribution of iron was apparent in the knock-outs. For example, decreases in Prussian blue staining of bone marrow along with increases in Prussian blue staining of the liver were observed (supplemental Fig. 4A-B). Taken together, these data suggest that increased oxidative stress in cells of hematopoietic lineages results in a redistribution of iron stores to the spleen and liver.

To examine whether the increase in splenic iron had any functional consequences on the spleen, genes possessing iron regulatory elements (IRE) were examined in spleens of *Sod2*$^{L/L}$ and *Sod2*$^{-/-}$ animals. Two to four fold increases in the mRNAs of aminolevulinate synthase 2 (ALAS2), heavy-chain ferritin (Fer H), light-chain ferritin (Fer L), and transferrin

receptor (TfR) were observed in the spleens of knockout animals (Fig. 4A). These findings were carried through to the protein level as well (Fig. 4B). Aforementioned, these genes possess IRE's which stabilize their mRNA transcripts in the presence of increased labile iron. Of note, while the thymus was devoid of *Sod2* protein and demonstrated increased oxidative stress there was no accumulation in iron noted (data not shown), and as expected the IRE regulated genes were not changed (Fig. 4B). Overall, these results further support increased iron redistribution to the spleen and alteration in iron homeostasis within animals that possessed a hematopoietic specific deletion of *Sod2*.

While the *Sod2*$^{-/-}$ mice showed a loss of normal iron homeostasis due to the loss of the anti-oxidant enzyme, the question remained as to what were the underlying molecular mechanism(s) responsible for this defect. We hypothesized that a heme biosynthetic defect might exist that could explain parts of the phenotype. Understanding that ferrochelatase (FECH) is an iron-sulfur cluster enzyme and sensitive to increases in nitric oxide, we investigated if FECH activity was sensitive to the increase in superoxide oxidative stress in *Sod2*$^{-/-}$ mice. By measuring the amount of zinc incorporated into deuteroporphyrin over time *in vitro*, it was observed that the *Sod2*$^{-/-}$ marrow had approximately 50% less FECH specific activity compared to *Sod2*$^{L/L}$ marrow with only a slight change in FECH protein levels (Fig. 5A-B). This finding correlated with our previous observation indicating a 50% decrease in hemoglobin in *Sod2*$^{-/-}$ peripheral blood (Fig. 2B). Additionally, an assay to measure total iron-free macrocycles demonstrated an approximate 10-fold increase in macrocycles in both the blood and feces of *Sod2*$^{-/-}$ mice (Fig. 5C). Furthermore, small but significant increases in macrocycles were noted in the plasma and urine. Taken together, these data suggest heme synthesis is at least impaired at the level of iron insertion to porphyrin by FECH, and may in part contribute to the observed phenotype in *Sod2*$^{-/-}$ mice.

Erythroid precursors from Sod2$^{-/-}$ animals exhibited aberrant fetal globin expression associated with global changes in histone modifications

Understanding that iron-responsive gene expression was increased in *Sod2*$^{-/-}$ mice, we investigated if the expression of iron-containing genes (*i.e.* globins) was also deregulated. Globin gene regulation throughout embryonic development and fetal to adult globin gene switching is a tightly regulated epigenetic process requiring a harmony of transcriptional and chromatin modifying events. Transcription factors including GATA1, GATA2, KLF1, and KLF2 play an integral role in this regulatory process of switching from primitive to adult forms of hemoglobin [41-45]. Using quantitative real-time PCR, we queried the steady-state levels of these transcription factors' mRNA in the spleens of our mice to determine whether mitochondrial oxidative stress could aberrantly affect their regulation. Notably, *Sod2*$^{-/-}$ mice demonstrated a complex pattern of expression of these transcription factors that was significantly different from their littermate controls (Fig. 6A). This pattern of expression is consistent with accelerated erythropoiesis, as increased KLF1 and GATA1 cooperatively govern erythrocyte maturation [46-48]. Additionally, the concurrent decreases in KLF2 and GATA2 were anticipated as KLF1 and GATA1 negatively regulate of these genes respectively [41, 49-51]. In contrast to these expected results, when quantifying the specific globins within the same organ it was found that essentially all types of globins (*i.e.* fetal and adult) were expressed to a greater extent in the *Sod2*$^{-/-}$ animals versus *Sod2*$^{L/L}$ (Fig. 6B-C). While the expression pattern of erythropoietic transcription factors and extramedullary hematopoiesis could partially explain the increase in adult globins (*e.g.* α1, α2, β Maj, β Min), these pro-erythropoietic events cannot explain the loss of silencing of fetal globins (*e.g.* HBq1, ζ, γε, h1) in *Sod2*$^{-/-}$ adult animals.

The process of switching from fetal to adult globins has been extensively described as an epigenetic process regulated primarily by an array of histone modifications [52-55]. Because of the aberrant fetal globin expression and apparent failure to switch off fetal globins during

erythroid maturation, it was hypothesized that oxidative stress contributed to a loss of epigenetic control in erythropoietic development in the *Sod2*$^{-/-}$ animals. To test this hypothesis, splenic nuclear protein from *Sod2*$^{L/L}$ and *Sod2*$^{-/-}$ animals was probed for various histone modifications known to regulate globin switching (Fig. 6D-E). Our results indicate that loss of *Sod2* in erythroid precursors is associated with a global decrease in histone modifications including methylation and acetylation. The profound alteration of global histone modifications observed correlates with the transcriptional deregulation throughout the spleen, and may explain at least in part the abnormal expression of fetal globin chains.

Mitochondrially targeted anti-oxidants rescue the oxidative stress induced erythrocyte defects

The conditional loss of *Sod2*$^{-/-}$ in hematopoietic lineages has produced a mouse model with significant pathology. With this model we aimed to query the effects of heme, N-acetyl cysteine (NAC), and mitochondrial targeted anti-oxidant (mito-tempol) therapies on the observed phenotype. To examine whether heme therapy would rescue the effects on *Sod2*$^{-/-}$ mice, hemin administration was performed. The rationale for this rescue was that a simple replacement of heme may counteract the aberrant production observed in the *Sod2*$^{-/-}$ animals. In *Sod2*$^{-/-}$ mice, hemin was able to partially rescue the defects in hemoglobin and hematocrit. In addition, hemin administration resulted in an approximate 50% decrease in circulating reticulocytes (Fig. 7A). These data further support the evidence of a heme synthesis aberration in *Sod2*$^{-/-}$ mice, since the acquisition of fully formed heme (by hemin) appeared to be utilized efficiently in the formation of hemoglobin and functional erythrocytes.

Next, we attempted to rescue the heme defect in *Sod2*$^{-/-}$ mice by the use of N-acetyl cysteine (NAC). NAC, a clinically approved agent, functions to replete glutathione pools and aid in two electron antioxidant reduction reactions [56]. We hypothesized that due to the abundance of labile iron and superoxide that increased hydrogen peroxide (by Fenton chemistry) may be formed, which NAC would function to eliminate. Unfortunately, NAC did not have any significant effect on restoring the heme defect as demonstrated by no change in hemoglobin or hematocrit in the knock-outs (Fig. 7A). Interestingly, NAC administration did decrease reticulocytes to similar levels as the hemin rescue. These data suggest the observed anemia in *Sod2*$^{-/-}$ mice possibly is due to a combination of at least two factors: 1) decreased heme synthesis, and 2) cellular damage elicited by oxidative stress. NAC may have beneficial effects on the latter, but no consequence on the former. Our dosing regimen was chosen on the basis of previously reported antioxidant effects [33, 34], but NAC has been shown to be both pro- and anti-oxidant depending upon concentration [57, 58]. Further studies examining different dosing ranges of NAC would be needed to fully understand the contribution of this drug in our system. Additionally, NAC has been shown in certain systems to slow cell cycle progression [59], as such in this model NAC may not be eliciting a beneficial antioxidant effect but rather limiting the production of new erythroid progenitors. Overall, the data presented here suggest NAC displays confounding results in the reversion of the *Sod2*$^{-/-}$ phenotype, but we cannot rule out its therapeutic potential in this model at this time.

Finally, because of the common cellular location of *Sod2* activity and FECH-mediated heme synthesis in the mitochondrial matrix, it was reasoned that specific mitochondrial targeted anti-oxidant therapies may be able to reverse the heme defect in *Sod2*$^{-/-}$ mice. Mito-tempol is a nitroxide that has reactivity as a superoxide dismutase mimetic; it also has a lipophilic tri-phenyl phosphonium cation moiety that targets anti-oxidant to the mitochondria. Furthermore, nitroxide anti-oxidants primarily function in one electron antioxidant reactions, which may be of increased benefit than NAC due to the previously discussed increase in superoxide in our model. Administration of mito-tempol provided a significant increase in

hemoglobin and hematocrit, as well as a decrease in reticulocytes; a partial rescue similar to hemin treatment (Fig. 7A). Furthermore, mito-tempol was able to significantly lower thiobarbituric acid reactive substances (TBARS), suggesting a limited amelioration of oxidative stress induced damage upon treatment with a mitochondrially targeted antioxidant molecule (Fig. 7B). These data imply that increased mitochondrial superoxide is specifically and causally involved in the propagation of the phenotype observed in mice with *Sod2*$^{-/-}$ deficient hematopoietic stem cells, and that suppression of elevated levels of mitochondrial superoxide may limit the hematopoietic defect and improve circulating red blood cell function.

DISCUSSION

In 2001, Friedman *et al.* created a marrow-deficient *Sod2* mouse model by lethal irradiation of a host mouse followed by subsequent transplantation of *Sod2*$^{-/-}$ fetal murine liver stem cells capable of hematopoiesis [60, 61]. In depth analysis of these animals identified an apparent sideroblastic anemia (SA) phenotype. The model of hematopoietic *Sod2* loss described herein significantly extends these findings by elucidating a deregulation of iron homeostasis which may be due in part to increased mitochondrial oxidative stress. Additionally, Friedman *et al.* observed a partial rescue of the described SA phenotype by the use of an anti-oxidant molecule (*i.e.* EUK-8). EUK-8 is a salen-manganese complex that has been shown to possess both superoxide dismutase (one-electron) and catalase activity (two-electron) [62, 63]. These results augment our own in that we demonstrate a weak partial rescue using a non-targeted two-electron anti-oxidant (*i.e.* NAC), and a more significant amelioration of the *Sod2*$^{-/-}$ pathogenesis using a mitochondrially-targeted one-electron anti-oxidant (*i.e.* mito-tempol). Using various methods of detection, we illustrate that the one-electron pro-oxidant superoxide is the most abundant ROS in *Sod2*$^{-/-}$ hematopoietic tissues, which explains the increased efficiency of mito-tempol versus NAC. Our examination of these anti-oxidants separately furthers the understanding that mitochondrially-targeted one-electron donors are more efficient in the attenuation of the *Sod2*$^{-/-}$ phenotype.

The use of the vav-iCre creates a highly efficient and specific knock-out of *Sod2* in the hematopoietic compartment of our mice. It is of note that the vav promoter does not become active within the embryonic yolk sac, and is activated in the fetal liver on day 11.5-12.5 of development [37]. This limitation of our model precludes any determination of the role of *Sod2* in primitive erythropoiesis, but this may prove difficult to study as no promoter to our knowledge specifically targets the hematopoietic compartment earlier in development than vav. The use of a promoter that is expressed earlier in development may lead to more constitutive expression of Cre, and thus off-target effects of *Sod2* deletion. As previously discussed, the constitutive *Sod2* knock-out mouse succumbs to multiple organ failure shortly after birth, and this finding is attributed to the inability of the specific tissues to compensate for the increase in superoxide [6, 7]. In contrast, we and others have demonstrated that sensitive tissues in the constitutive *Sod2* knock-out showed limited to undetectable phenotypes when specifically targeted for *Sod2* deletion [28, 64, 65]. With the findings presented here that FECH activity is inhibited when *Sod2* is removed from the hematopoietic compartment (and potentially other tissues), we put forth the hypothesis that the impairment of heme synthesis by increased superoxide may be an additional contribution to the premature death noted in the constitutive *Sod2* knock-out mouse.

The results presented here demonstrate that increases in the steady-state levels of mitochondrial superoxide have the ability to impair FECH activity, which extends the findings of FECH inactivation by a different free radical, nitric oxide. While superoxide may directly inactivate FECH by disruption of its 2Fe/2S cluster, the inactivation may be simply due to removal of bioavailable ferrous iron [17]. Superoxide has long been described to have

the ability to inactivate certain Fe-S cluster enzymes such as aconitase and succinate dehydrogenase [39, 66]. We demonstrate a significant inhibition of aconitase activity in the *Sod2*$^{-/-}$ hematopoietic tissues. In these assays, we did not separate mitochondrial and cytosolic fractions, and as such our assay reflects total, or both aconitase 1 and 2 activities. Aconitase 2 is mitochondrally located, and participates in the citric acid cycle. Aconitase 1, also known as iron regulatory protein 1, is present in the cytosol and is involved in both citrate conversion and cellular iron maintenance. Inactivation of either or both of these isoforms could have significant impacts on iron homeostasis, which we observe in the *Sod2*$^{-/-}$ animals. Furthermore, these metabolic enzymes possess a characteristic 4Fe/4S cluster arrangement, which is quite diverse from the 2Fe/2S organization of FECH. Further studies would be necessary to understand the comparative inactivation of all of these Fe/S containing enzymes (in addition to other mitochondrially-located heme synthesis enzymes) by superoxide, which could elucidate the differential sensitivity of targets within stressed mitochondria.

The *Sod2*$^{-/-}$ mice demonstrated a robust increase in erythropoietin produced in the kidneys, suggesting a systemic hypoxia within these animals. Oxygen tension has been demonstrated to play a significant role in globin regulatory processes (which may play a significant role in *Sod2*$^{-/-}$ mice due to abundant hematopoietic superoxide and increased systemic hypoxia). Various models of erythrocyte development show aberrant globin switching patterns whether exposed to normoxia versus hypoxia [71, 72]. These changes may be due in part to the hypoxia inducible factor (HIF), but the limited transcriptional capabilities of HIF cannot fully explain the entire process of mammalian erythrocyte development or the complex gene expression pattern noted in the *Sod2*$^{-/-}$ animals.

The process of globin switching throughout mammalian erythrocyte development is a tightly regulated epigenetic process. Transcription factors, histone modifications, and recently discovered DNA methylation all have significant parts in the control of this process [41, 42, 67, 68]. Most of the epigenetic modifying enzymes require cofactors to function, and many of these cofactors are derived from cellular metabolism [69, 70]. This inherent dependency on metabolic cofactors creates a connection between cellular metabolism and gene regulation that is not yet fully understood [69]. In the *Sod2*$^{-/-}$ mouse model presented here, it is demonstrated that an increase in steady-state superoxide leads to a disruption of both metabolic enzymes and iron homeostasis; mitochondrial effects that have significant consequences on certain nuclear epigenetic modifying enzymes. For example, disruption of succinate dehydrogenase by superoxide could lead to a build-up of succinate. This metabolite can disrupt 2-oxoglutarate dependent dioxygenases (*e.g.* prolyl hydroxylases, jumonji histone demethylases, Tet DNA demethylases, etc.) that have both direct and indirect mechanisms of genetic regulation through epigenetic modification [26]. Furthermore, these nuclear enzymes require iron in the reduced form (Fe^{2+}) to properly function, thus loss of normal iron homeostasis in the *Sod2*$^{-/-}$ mouse may also have a significant impact on the functionality of these enzymes [73, 74]. Additionally, many cofactors of epigenetic modifying enzymes are redox sensitive, and as such a change in the GSH/GSSG, Fe^{2+}/Fe^{3+}, or NAD^{+}/NADH pools may elicit negative effects on these enzymes [69]. Last, genes implicated in regulation of nuclear-encoded mitochondrial genes may also be affected by the disruption of *Sod2* loss in the mitochondria. One of these genes, peroxisome proliferator-activated receptor gamma co-activator-related protein 1, has been shown to be up-regulated in a similar model of *Sod2* loss [75], and as such may also contribute to changes in gene expression observed in the *Sod2*$^{-/-}$ mice described here. Taking all of these mechanisms into account, it would be hypothesized that the epigenetic dysregulation in the *Sod2*$^{-/-}$ mice would have both increased and decreased epigenetic modifications, yet in our analysis here we only observed global decreases (in both activating and repressing histone marks). This important finding suggests that while interruption of the

aforementioned epigenetic regulatory enzymes plays a role in this model, the availability of co-factors necessary for methylation and acetylation (*e.g.* s-adenosylmethionine, acetyl-coA, etc.) may also be altered due to the observed metabolic disturbances. Metabolomic analysis in the *Sod2*$^{-/-}$ hematopoietic cells is highly warranted to understand nature of the metabolic disruption and its role in the epigenetic perturbation. Overall, the significant increase of mitochondrial superoxide and disruption of iron homeostasis predisposes the hematopoietic system to nuclear epigenetic changes, which participate in the observed loss of proper gene expression. Further understanding how the mitochondrial redox environment affects the control of nuclear gene expression through alterations in activating and repressing chromatin modifications may lead to novel therapeutic targets for genes that have been pathologically epigenetically expressed or silenced in disease. Such knowledge would be particularly well suited and translationally relevant to myelodysplastic syndrome where DNA methyltransferase (DNMT) inhibition with decitabine therapy is routinely prescribed.

Taken together the results presented here demonstrate, for the first time to our knowledge, that elevated steady-state levels of mitochondrial superoxide inhibit FECH enzyme activity *in vivo*. The disruption of the superoxide balance within the mitochondria leads to a cascade of molecular pathophysiologies including improper heme formation, gene regulation, and erythrocyte development. In addition, our results showed the beneficial therapeutic effect of supplementation with a single mitochondrially targeted anti-oxidant. Taken together, these exciting new findings clearly warrant further investigation of the redox control of erythrocyte development, and the potential of anti-oxidant therapies in hematopoietic pathologies that disrupt normal iron homeostasis.

Supplementary Material

Refer to Web version on PubMed Central for supplementary material.

Acknowledgments

We thank the University of Iowa Comparative Pathology Laboratory for their help in histology and analysis. We also thank The University of Iowa Flow Cytometry Facilities for their services. In addition, Dr. Adam Dupuy for his gracious donation of the Vav-iCre mouse strain.

FINANCIAL DISCLOSURE

This work was supported by the following grants: NIH RO1 CA073612, NIH RO1 CA115438, DOD PC073831, NIH P30 CA086862, and NIH T32 CA078586. The funders had no role in study design, data collection and analysis, decision to publish, or preparation of the manuscript.

ABBREVIATIONS

ROS	reactive oxygen species
$O_2^{\bullet-}$	superoxide
Sod2	manganese superoxide dismutase
FECH	ferrochelatase
Fe/S	iron-sulfur
$NO^{\bullet}$	nitric oxide
IRE	iron response element
DHE	dihydroethidium
TBARS	thiobarbituric acid reactive substances

NAC	N-acetyl cysteine
RNS	reactive nitrogen species
CBC	complete blood count
EMH	extramedullary hematopoiesis
EPO	erythropoietin
ALT	alanine aminotransferase
AST	aspartate aminotransferase
Fer H	ferritin heavy chain
Fer L	ferritin light chain
TfR	transferrin receptor
HIF	hypoxia inducible factor

REFERENCES

1. Fridovich I. The biology of oxygen radicals. Science. 1978; 201:875–880. [PubMed: 210504]
2. Fridovich I. Oxygen toxicity: a radical explanation. J Exp Biol. 1998; 201:1203–1209. [PubMed: 9510531]
3. Gius D, Spitz DR. Redox signaling in cancer biology. Antioxid Redox Signal. 2006; 8:1249–1252. [PubMed: 16910772]
4. Hensley K, Robinson KA, Gabbita SP, Salsman S, Floyd RA. Reactive oxygen species, cell signaling, and cell injury. Free Radic Biol Med. 2000; 28:1456–1462. [PubMed: 10927169]
5. Case AJ, McGill JL, Tygrett LT, Shirasawa T, Spitz DR, Waldschmidt TJ, Legge KL, Domann FE. Elevated mitochondrial superoxide disrupts normal T cell development, impairing adaptive immune responses to an influenza challenge. Free Radic Biol Med. 2011; 50:448–458. [PubMed: 21130157]
6. Lebovitz RM, Zhang H, Vogel H, Cartwright J Jr. Dionne L, Lu N, Huang S, Matzuk MM. Neurodegeneration, myocardial injury, and perinatal death in mitochondrial superoxide dismutase-deficient mice. Proc Natl Acad Sci U S A. 1996; 93:9782–9787. [PubMed: 8790408]
7. Li Y, Huang TT, Carlson EJ, Melov S, Ursell PC, Olson JL, Noble LJ, Yoshimura MP, Berger C, Chan PH, Wallace DC, Epstein CJ. Dilated cardiomyopathy and neonatal lethality in mutant mice lacking manganese superoxide dismutase. Nat Genet. 1995; 11:376–381. [PubMed: 7493016]
8. Ajioka RS, Phillips JD, Kushner JP. Biosynthesis of heme in mammals. Biochim Biophys Acta. 2006; 1763:723–736. [PubMed: 16839620]
9. Fenton H. Oxidation of tartaric acid in the presence of iron. J. Chem. Soc., Trans. 1894; 65:11.
10. Haber F, Weiss J. The Catalytic Decomposition of Hydrogen Peroxide by Iron Salts. Proceedings of the Royal Society of London. Series A - Mathematical and Physical Sciences. 1934; 147:332–351.
11. Kruszewski M. Labile iron pool: the main determinant of cellular response to oxidative stress. Mutation research. 2003; 531:81–92. [PubMed: 14637247]
12. Greenberg GR, Wintrobe MM. A labile iron pool. J Biol Chem. 1946; 165:397. [PubMed: 21001229]
13. Brazzolotto X, Gaillard J, Pantopoulos K, Hentze MW, Moulis JM. Human cytoplasmic aconitase (Iron regulatory protein 1) is converted into its [3Fe-4S] form by hydrogen peroxide in vitro but is not activated for iron-responsive element binding. J Biol Chem. 1999; 274:21625–21630. [PubMed: 10419470]
14. Gardner PR, Fridovich I. Superoxide sensitivity of the Escherichia coli aconitase. J Biol Chem. 1991; 266:19328–19333. [PubMed: 1655783]

15. Wu CK, Dailey HA, Rose JP, Burden A, Sellers VM, Wang BC. The 2.0 A structure of human ferrochelatase, the terminal enzyme of heme biosynthesis. Nature structural biology. 2001; 8:156–160.
16. Dailey HA, Finnegan MG, Johnson MK. Human ferrochelatase is an iron-sulfur protein. Biochemistry. 1994; 33:403–407. [PubMed: 8286370]
17. Crooks DR, Ghosh MC, Haller RG, Tong WH, Rouault TA. Posttranslational stability of the heme biosynthetic enzyme ferrochelatase is dependent on iron availability and intact iron-sulfur cluster assembly machinery. Blood. 2010; 115:860–869. [PubMed: 19965627]
18. Dailey HA, Dailey TA, Wu CK, Medlock AE, Wang KF, Rose JP, Wang BC. Ferrochelatase at the millennium: structures, mechanisms and [2Fe-2S] clusters. Cell Mol Life Sci. 2000; 57:1909–1926. [PubMed: 11215517]
19. Furukawa T, Kohno H, Tokunaga R, Taketani S. Nitric oxide-mediated inactivation of mammalian ferrochelatase in vivo and in vitro: possible involvement of the iron-sulphur cluster of the enzyme. Biochem J. 1995; 310(Pt 2):533–538. [PubMed: 7544575]
20. Kim YM, Bergonia HA, Muller C, Pitt BR, Watkins WD, Lancaster JR Jr. Loss and degradation of enzyme-bound heme induced by cellular nitric oxide synthesis. J Biol Chem. 1995; 270:5710–5713. [PubMed: 7890697]
21. Boveris, A.; Cadenas, E. Cellular sources and steady-state levels of reactive oxygen species. New York: 1997.
22. Chance B, Sies H, Boveris A. Hydroperoxide metabolism in mammalian organs. Physiol Rev. 1979; 59:527–605. [PubMed: 37532]
23. Bize IB, Oberley LW, Morris HP. Superoxide dismutase and superoxide radical in Morris hepatomas. Cancer Res. 1980; 40:3686–3693. [PubMed: 6254638]
24. Slane BG, Aykin-Burns N, Smith BJ, Kalen AL, Goswami PC, Domann FE, Spitz DR. Mutation of succinate dehydrogenase subunit C results in increased O2.-, oxidative stress, and genomic instability. Cancer Res. 2006; 66:7615–7620. [PubMed: 16885361]
25. Forman HJ, Kennedy JA. Role of superoxide radical in mitochondrial dehydrogenase reactions. Biochemical and biophysical research communications. 1974; 60:1044–1050. [PubMed: 4372996]
26. Smith EH, Janknecht R, Maher LJ 3rd. Succinate inhibition of alpha-ketoglutarate-dependent enzymes in a yeast model of paraganglioma. Human molecular genetics. 2007; 16:3136–3148. [PubMed: 17884808]
27. Sasaki M, Knobbe CB, Munger JC, Lind EF, Brenner D, Brustle A, Harris IS, Holmes R, Wakeham A, Haight J, You-Ten A, Li WY, Schalm S, Su SM, Virtanen C, Reifenberger G, Ohashi PS, Barber DL, Figueroa ME, Melnick A, Zuniga-Pflucker JC, Mak TW. IDH1(R132H) mutation increases murine haematopoietic progenitors and alters epigenetics. Nature. 2012; 488:656–659. [PubMed: 22763442]
28. Ikegami T, Suzuki Y, Shimizu T, Isono K, Koseki H, Shirasawa T. Model mice for tissue-specific deletion of the manganese superoxide dismutase (MnSOD) gene. Biochemical and biophysical research communications. 2002; 296:729–736. [PubMed: 12176043]
29. de Boer J, Williams A, Skavdis G, Harker N, Coles M, Tolaini M, Norton T, Williams K, Roderick K, Potocnik AJ, Kioussis D. Transgenic mice with hematopoietic and lymphoid specific expression of Cre. Eur J Immunol. 2003; 33:314–325. [PubMed: 12548562]
30. Poh-Fitzpatrick MB, Piomelli S, Young P, Hsu H, Harber LC. Rapid quantitative assay for erythrocyte porphyrins. Arch Dermatol. 1974; 110:225–230. [PubMed: 4854030]
31. Choi KM, Gibbons SJ, Nguyen TV, Stoltz GJ, Lurken MS, Ordog T, Szurszewski JH, Farrugia G. Heme oxygenase-1 protects interstitial cells of Cajal from oxidative stress and reverses diabetic gastroparesis. Gastroenterology. 2008; 135:2055–2064. e2051–2052. 2064. [PubMed: 18926825]
32. Kirino M, Kirino Y, Takeno M, Nagashima Y, Takahashi K, Kobayashi M, Murakami S, Hirasawa T, Ueda A, Aihara M, Ikezawa Z, Ishigatsubo Y. Heme oxygenase 1 attenuates the development of atopic dermatitis-like lesions in mice: implications for human disease. The Journal of allergy and clinical immunology. 2008; 122:290–297. e291–298. 297. [PubMed: 18582925]
33. Ercal N, Neal R, Treeratphan P, Lutz PM, Hammond TC, Dennery PA, Spitz DR. A role for oxidative stress in suppressing serum immunoglobulin levels in lead-exposed Fisher 344 rats.

Archives of environmental contamination and toxicology. 2000; 39:251–256. [PubMed: 10871428]

34. Morrison JP, Coleman MC, Aunan ES, Walsh SA, Spitz DR, Kregel KC. Thiol supplementation in aged animals alters antioxidant enzyme activity after heat stress. Journal of applied physiology. 2005; 99:2271–2277. [PubMed: 16099896]
35. Khan SA, Nanduri J, Yuan G, Kinsman B, Kumar GK, Joseph J, Kalyanaraman B, Prabhakar NR. NADPH oxidase 2 mediates intermittent hypoxia-induced mitochondrial complex I inhibition: relevance to blood pressure changes in rats. Antioxid Redox Signal. 2011; 14:533–542. [PubMed: 20618070]
36. Ogilvy S, Elefanty AG, Visvader J, Bath ML, Harris AW, Adams JM. Transcriptional regulation of vav, a gene expressed throughout the hematopoietic compartment. Blood. 1998; 91:419–430. [PubMed: 9427694]
37. Ogilvy S, Metcalf D, Gibson L, Bath ML, Harris AW, Adams JM. Promoter elements of vav drive transgene expression in vivo throughout the hematopoietic compartment. Blood. 1999; 94:1855–1863. [PubMed: 10477714]
38. Robinson KM, Janes MS, Pehar M, Monette JS, Ross MF, Hagen TM, Murphy MP, Beckman JS. Selective fluorescent imaging of superoxide in vivo using ethidium-based probes. Proc Natl Acad Sci U S A. 2006; 103:15038–15043. [PubMed: 17015830]
39. Gardner PR, Fridovich I. Inactivation-reactivation of aconitase in Escherichia coli. A sensitive measure of superoxide radical. J Biol Chem. 1992; 267:8757–8763. [PubMed: 1315737]
40. Tortora V, Quijano C, Freeman B, Radi R, Castro L. Mitochondrial aconitase reaction with nitric oxide, S-nitrosoglutathione, and peroxynitrite: mechanisms and relative contributions to aconitase inactivation. Free Radic Biol Med. 2007; 42:1075–1088. [PubMed: 17349934]
41. Alhashem YN, Vinjamur DS, Basu M, Klingmuller U, Gaensler KM, Lloyd JA. Transcription factors KLF1 and KLF2 positively regulate embryonic and fetal beta-globin genes through direct promoter binding. J Biol Chem. 2011; 286:24819–24827. [PubMed: 21610079]
42. Fujiwara Y, Chang AN, Williams AM, Orkin SH. Functional overlap of GATA-1 and GATA-2 in primitive hematopoietic development. Blood. 2004; 103:583–585. [PubMed: 14504093]
43. Pevny L, Simon MC, Robertson E, Klein WH, Tsai SF, D'Agati V, Orkin SH, Costantini F. Erythroid differentiation in chimaeric mice blocked by a targeted mutation in the gene for transcription factor GATA-1. Nature. 1991; 349:257–260. [PubMed: 1987478]
44. Siatecka M, Bieker JJ. The multifunctional role of EKLF/KLF1 during erythropoiesis. Blood. 2011; 118:2044–2054. [PubMed: 21613252]
45. Tsai FY, Keller G, Kuo FC, Weiss M, Chen J, Rosenblatt M, Alt FW, Orkin SH. An early haematopoietic defect in mice lacking the transcription factor GATA-2. Nature. 1994; 371:221–226. [PubMed: 8078582]
46. Pilon AM, Ajay SS, Kumar SA, Steiner LA, Cherukuri PF, Wincovitch S, Anderson SM, Center NCS, Mullikin JC, Gallagher PG, Hardison RC, Margulies EH, Bodine DM. Genome-wide ChIP-Seq reveals a dramatic shift in the binding of the transcription factor erythroid Kruppel-like factor during erythrocyte differentiation. Blood. 2011; 118:e139–148. [PubMed: 21900194]
47. Tallack MR, Whitington T, Yuen WS, Wainwright EN, Keys JR, Gardiner BB, Nourbakhsh E, Cloonan N, Grimmond SM, Bailey TL, Perkins AC. A global role for KLF1 in erythropoiesis revealed by ChIP-seq in primary erythroid cells. Genome research. 2010; 20:1052–1063. [PubMed: 20508144]
48. Zhou D, Pawlik KM, Ren J, Sun CW, Townes TM. Differential binding of erythroid Krupple-like factor to embryonic/fetal globin gene promoters during development. J Biol Chem. 2006; 281:16052–16057. [PubMed: 16606611]
49. Dore LC, Chlon TM, Brown CD, White KP, Crispino JD. Chromatin occupancy analysis reveals genome-wide GATA factor switching during hematopoiesis. Blood. 2012
50. Ikonomi P, Noguchi CT, Miller W, Kassahun H, Hardison R, Schechter AN. Levels of GATA-1/GATA-2 transcription factors modulate expression of embryonic and fetal hemoglobins. Gene. 2000; 261:277–287. [PubMed: 11167015]
51. Vicente C, Conchillo A, Garcia-Sanchez MA, Odero MD. The role of the GATA2 transcription factor in normal and malignant hematopoiesis. Critical reviews in oncology/hematology. 2011

52. Burns LJ, Glauber JG, Ginder GD. Butyrate induces selective transcriptional activation of a hypomethylated embryonic globin gene in adult erythroid cells. Blood. 1988; 72:1536–1542. [PubMed: 2460154]
53. Fu XH, Liu DP, Tang XB, Liu G, Lv X, Li YJ, Liang CC. A conserved, extended chromatin opening within alpha-globin locus during development. Experimental cell research. 2005; 309:174–184. [PubMed: 16002065]
54. Ishiguro K, Sartorelli AC. Coinduction of embryonic and adult-type globin mRNAs by sodium butyrate and trichostatin A in two murine interleukin-3-dependent bone marrow-derived cell lines. Blood. 1998; 92:4383–4393. [PubMed: 9834245]
55. Yin W, Barkess G, Fang X, Xiang P, Cao H, Stamatoyannopoulos G, Li Q. Histone acetylation at the human beta-globin locus changes with developmental age. Blood. 2007; 110:4101–4107. [PubMed: 17881636]
56. Atkuri KR, Mantovani JJ, Herzenberg LA. N-Acetylcysteine--a safe antidote for cysteine/glutathione deficiency. Curr Opin Pharmacol. 2007; 7:355–359. [PubMed: 17602868]
57. Hadzic T, Li L, Cheng N, Walsh SA, Spitz DR, Knudson CM. The role of low molecular weight thiols in T lymphocyte proliferation and IL-2 secretion. J Immunol. 2005; 175:7965–7972. [PubMed: 16339532]
58. Sagara J, Bannai S, Shikano N, Makino N. Conflicting effects of N-acetylcysteine on purified neurons derived from rat cortical culture. Neuroreport. 2010; 21:416–421. [PubMed: 20838280]
59. Menon SG, Sarsour EH, Spitz DR, Higashikubo R, Sturm M, Zhang H, Goswami PC. Redox regulation of the G1 to S phase transition in the mouse embryo fibroblast cell cycle. Cancer Res. 2003; 63:2109–2117. [PubMed: 12727827]
60. Friedman JS, Lopez MF, Fleming MD, Rivera A, Martin FM, Welsh ML, Boyd A, Doctrow SR, Burakoff SJ. SOD2-deficiency anemia: protein oxidation and altered protein expression reveal targets of damage, stress response, and antioxidant responsiveness. Blood. 2004; 104:2565–2573. [PubMed: 15205258]
61. Friedman JS, Rebel VI, Derby R, Bell K, Huang TT, Kuypers FA, Epstein CJ, Burakoff SJ. Absence of mitochondrial superoxide dismutase results in a murine hemolytic anemia responsive to therapy with a catalytic antioxidant. J Exp Med. 2001; 193:925–934. [PubMed: 11304553]
62. Baudry M, Etienne S, Bruce A, Palucki M, Jacobsen E, Malfroy B. Salen-manganese complexes are superoxide dismutase-mimics. Biochemical and biophysical research communications. 1993; 192:964–968. [PubMed: 8484797]
63. Gonzalez PK, Zhuang J, Doctrow SR, Malfroy B, Benson PF, Menconi MJ, Fink MP. EUK-8, a synthetic superoxide dismutase and catalase mimetic, ameliorates acute lung injury in endotoxemic swine. The Journal of pharmacology and experimental therapeutics. 1995; 275:798–806. [PubMed: 7473169]
64. Case AJ, Domann FE. Manganese superoxide dismutase is dispensable for post-natal development and lactation in the murine mammary gland. Free radical research. 2012
65. Lustgarten M, Jang Y, Liu Y, Muller F, Qi W, Steinhelper M, Brooks S, Larkin LM, Shimizu T, Shirasawa T, McManus L, Bhattacharya A, Richardson A, Van Remmen H. Conditional knockout of MnSOD targeted to type IIB skeletal muscle fibers increases oxidative stress and is sufficient to alter aerobic exercise capacity. Am J Physiol Cell Physiol. 2009
66. Zhang Y, Marcillat O, Giulivi C, Ernster L, Davies KJ. The oxidative inactivation of mitochondrial electron transport chain components and ATPase. J Biol Chem. 1990; 265:16330–16336. [PubMed: 2168888]
67. De Gobbi M, Anguita E, Hughes J, Sloane-Stanley JA, Sharpe JA, Koch CM, Dunham I, Gibbons RJ, Wood WG, Higgs DR. Tissue-specific histone modification and transcription factor binding in alpha globin gene expression. Blood. 2007; 110:4503–4510. [PubMed: 17715390]
68. Shearstone JR, Pop R, Bock C, Boyle P, Meissner A, Socolovsky M. Global DNA demethylation during mouse erythropoiesis in vivo. Science. 2011; 334:799–802. [PubMed: 22076376]
69. Cyr A, Domann F. The Redox Basis of Epigenetic Modifications: From Mechanisms to Functional Consequences. Antioxid Redox Signal. 2010
70. Hitchler MJ, Domann FE. An epigenetic perspective on the free radical theory of development. Free Radic Biol Med. 2007; 43:1023–1036. [PubMed: 17761298]

71. Bichet S, Wenger RH, Camenisch G, Rolfs A, Ehleben W, Porwol T, Acker H, Fandrey J, Bauer C, Gassmann M. Oxygen tension modulates beta-globin switching in embryoid bodies. FASEB J. 1999; 13:285–295. [PubMed: 9973316]

72. Roesner A, Hankeln T, Burmester T. Hypoxia induces a complex response of globin expression in zebrafish (Danio rerio). J Exp Biol. 2006; 209:2129–2137. [PubMed: 16709914]

73. Flashman E, Davies SL, Yeoh KK, Schofield CJ. Investigating the dependence of the hypoxia-inducible factor hydroxylases (factor inhibiting HIF and prolyl hydroxylase domain 2) on ascorbate and other reducing agents. Biochem J. 2010; 427:135–142. [PubMed: 20055761]

74. Hirsila M, Koivunen P, Gunzler V, Kivirikko KI, Myllyharju J. Characterization of the human prolyl 4-hydroxylases that modify the hypoxia-inducible factor. J Biol Chem. 2003; 278:30772–30780. [PubMed: 12788921]

75. Martin FM, Xu X, von Lohneysen K, Gilmartin TJ, Friedman JS. SOD2 deficient erythroid cells up-regulate transferrin receptor and down-regulate mitochondrial biogenesis and metabolism. PLoS One. 2011; 6:e16894. [PubMed: 21326867]

HIGHLIGHTS

- The loss of *Sod2* in hematopoietic stem cells causes aberrant erythrocyte maturation
- Hematopoietic *Sod2* loss causes compensatory extramedullary hematopoiesis
- Iron homeostasis is disrupted systemically in conditional *Sod2* knock-out mice
- Increased mitochondrial oxidative stress leads to global epigenetic dysregulation
- Mitochondrially-targeted antioxidants rescue disruptions caused by *Sod2* loss

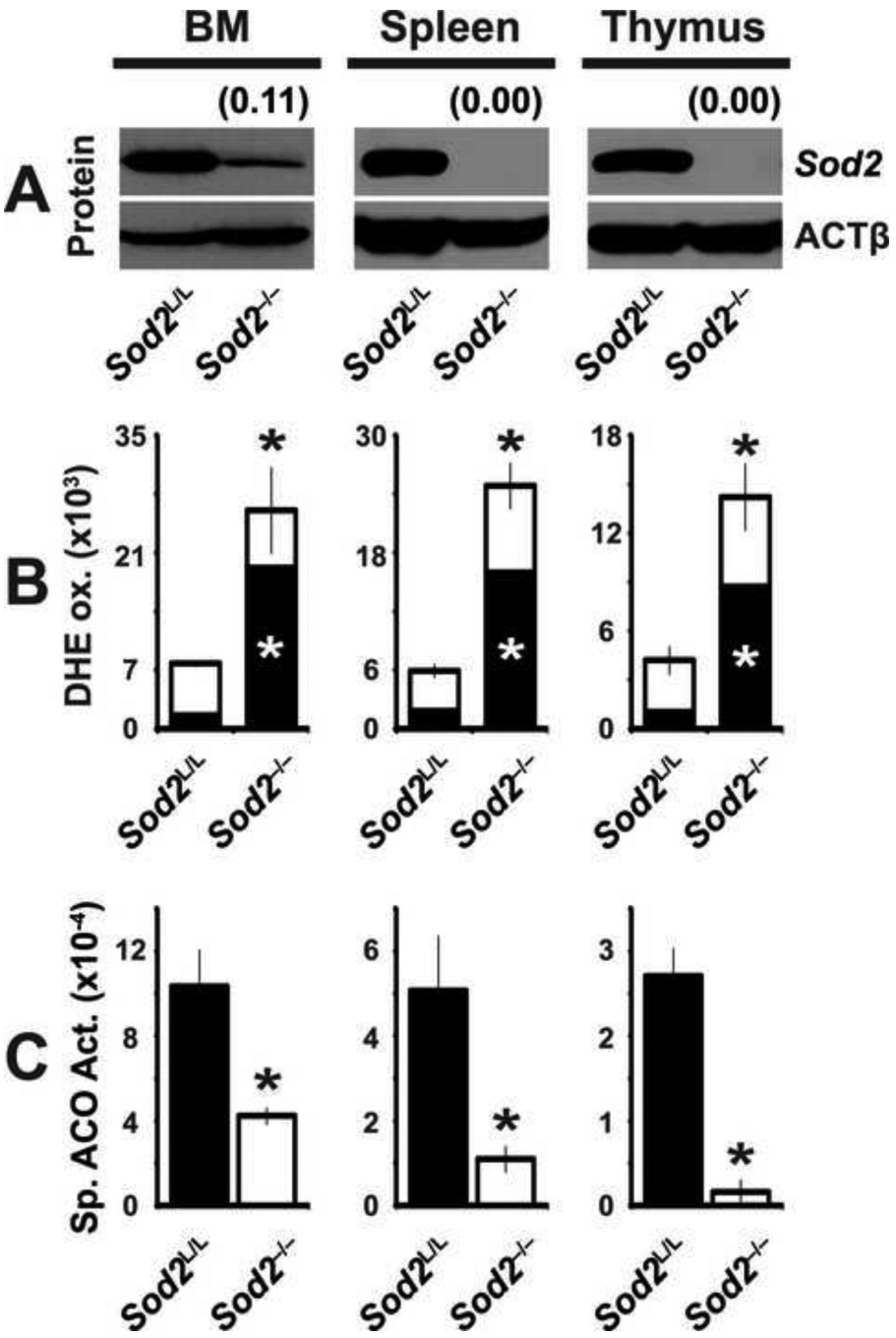

Figure. 1. Conditional loss of *Sod2* causes an increase in superoxide derived oxidative stress in hematopoietic tissues

(A) Western blot analysis for *Sod2* protein in hematopoietic tissues from 6-week old $Sod2^{L/L}$ or $Sod2^{-/-}$ mice. β-actin (ACTβ) shown as loading control. Quantification normalized to ACTβ, then to respective $Sod2^{L/L}$ tissue using ImageJ software. (B) Flow cytometric analysis of dihydroethidium (DHE) staining of respective hematopoietic tissues from 6-week old $Sod2^{L/L}$ or $Sod2^{-/-}$ mice. Quantification shown as total (488 nm excitation, 580 nm emission; entire bar) and superoxide specific (405 nm excitation, 580 nm emission; black section of bar) DHE staining. (C) Spectrophotometric analysis of total cellular aconitase (ACO) activity in hematopoietic tissues from 6-week old $Sod2^{L/L}$ or $Sod2^{-/-}$ mice.

Specific activity calculated based on relative ACO protein levels (supplemental Figure. 1B). Three mice of respective genotypes were analyzed per experiment; data are shown as mean and s.d. Where applicable, * = $p<0.01$ by Student's t-test versus $Sod2^{L/L}$.

A

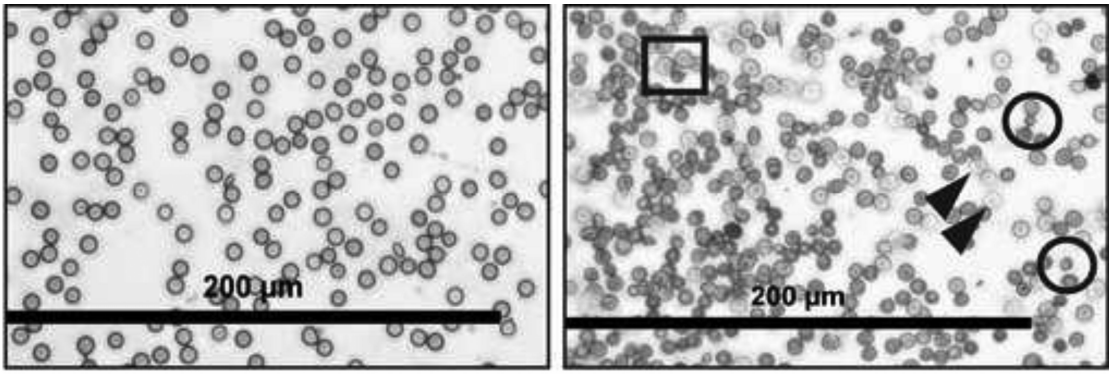

B

	Sod2 L/L	Sod2 −/−
RBC (cells/μL)	8.0 x 10^7 ± 1.0 x 10^6	5.8 x 10^7 ± 4.9 x 10^6 *
WBC (cells/μL)	1.02 x 10^4 ± 1.2 x 10^3	1.11 x 10^4 ± 1.9 x 10^3
Hgb (g/dL)	10.3 ± 0.6	4.7 ± 0.6 *
Hct (%)	41.0 ± 2.0	28.3 ± 1.5 *
Ret (%)	3.7 ± 0.8	30.4 ± 5.4 *
MCV (fL)	51.6 ± 1.8	49.6 ± 3.0
MCH (pg)	12.3 ± 0.3	8.3 ± 0.4 *
MCHC (g/dL)	23.9 ± 0.5	16.7 ± 1.5 *
CHCM (g/dL)	29.6 ± 0.3	26.9 ± 1.0 *
CH (g/dL)	15.3 ± 0.4	13.2 ± 0.3 *
RDW (%)	14.2 ± 2.0	21.6 ± 0.2 *
HDW (g/dL)	2.0 ± 0.1	3.5 ± 0.3 *
PLT (cells/μL)	1.4 x 10^6 ± 6.1 x 10^5	1.3 x 10^6 ± 1.1 x 10^5
MPV (fL)	5.83 ± 0.6	5.96 ± 0.5
Aniso	—	+++
Hypo	—	+++
HC Var	—	+++

Figure. 2. Elevated mitochondrial superoxide during erythropoiesis has damaging consequences on erythrocytes

(A) Wright-Giemsa stain of blood isolated from 6-week old *Sod2*$^{L/L}$ or *Sod2* $^{-/-}$ mice. Black rectangle indicates anisocytosis; black circles indicate spherocytosis; closed black arrowheads indicate hypochromatic cells. (B) Complete blood count analysis performed on peripheral blood from 6-week old *Sod2*$^{L/L}$ or *Sod2*$^{-/-}$ mice. RBC, red blood cells; WBC, white blood cells; Hgb, hemoglobin; Hct, hematocrit; Ret, reticulocytes; MCV, mean corpuscular volume; MCH, mean corpuscular hemoglobin; MCHC, mean corpuscular hemoglobin concentration; CHCM, cell hemoglobin concentration mean; CH, cellular hemoglobin; RDW, red blood cell distribution width; HDW, hemoglobin distribution width;

PLT, platelets; MPV, mean platelet volume; Aniso, anisocytosis; Hypo, hypochromasia; HC Var, hemoglobin concentration variance. Five mice of respective genotypes were analyzed per experiment; data are shown as mean and s.d. Where applicable, * = $p<0.01$ by Student's t-test versus *Sod2*$^{L/L}$.

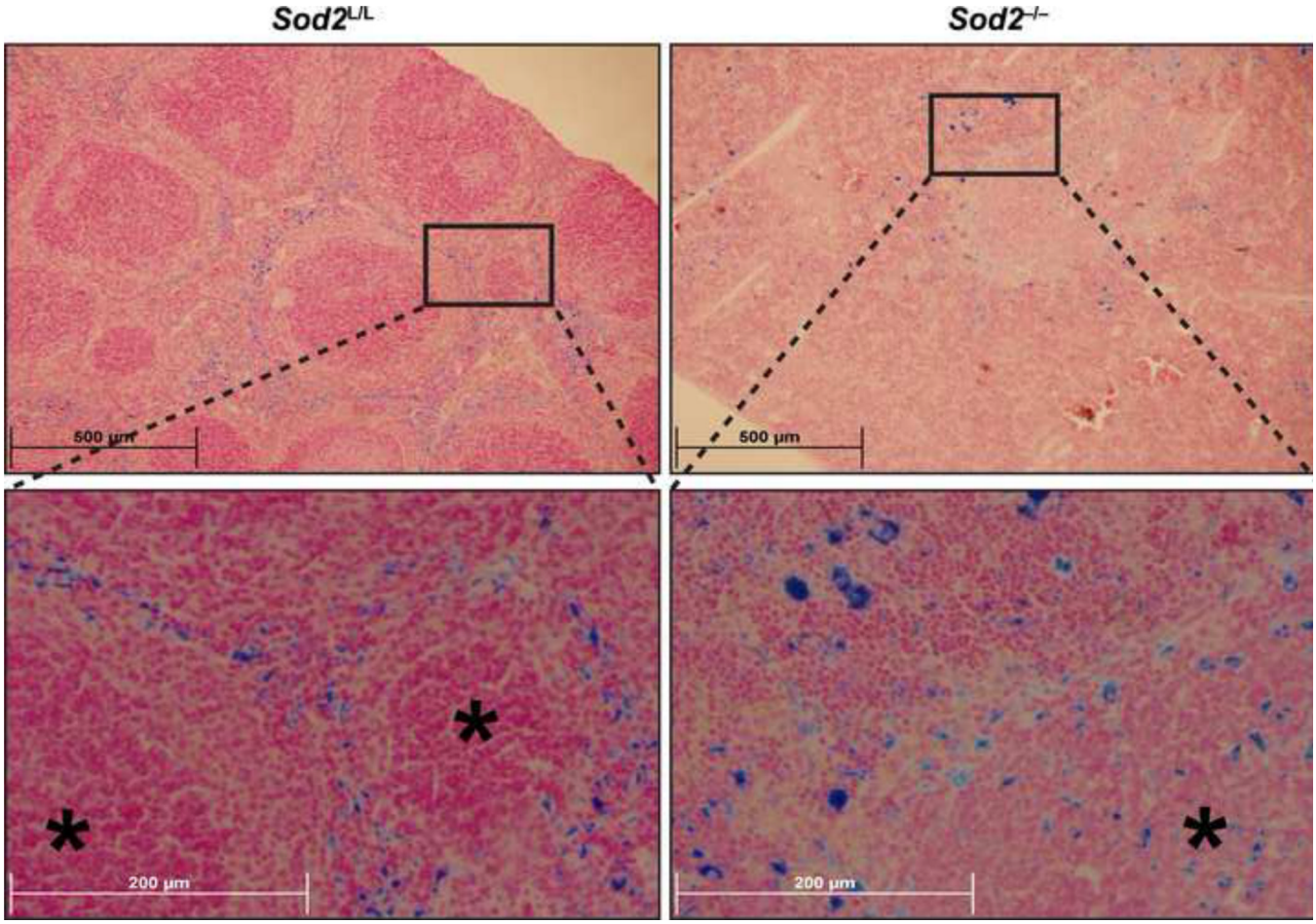

Figure. 3. *Sod2* deficient animals display aberrant hematopoietic iron metabolism

Upper panels - low magnification (10x) of Prussian blue stained 6-week old *Sod2*$^{L/L}$ or *Sod2*$^{-/-}$ spleens. Lower panels - high magnification (40x) of representative area in respective spleens. Asterisks indicate areas of white pulp.

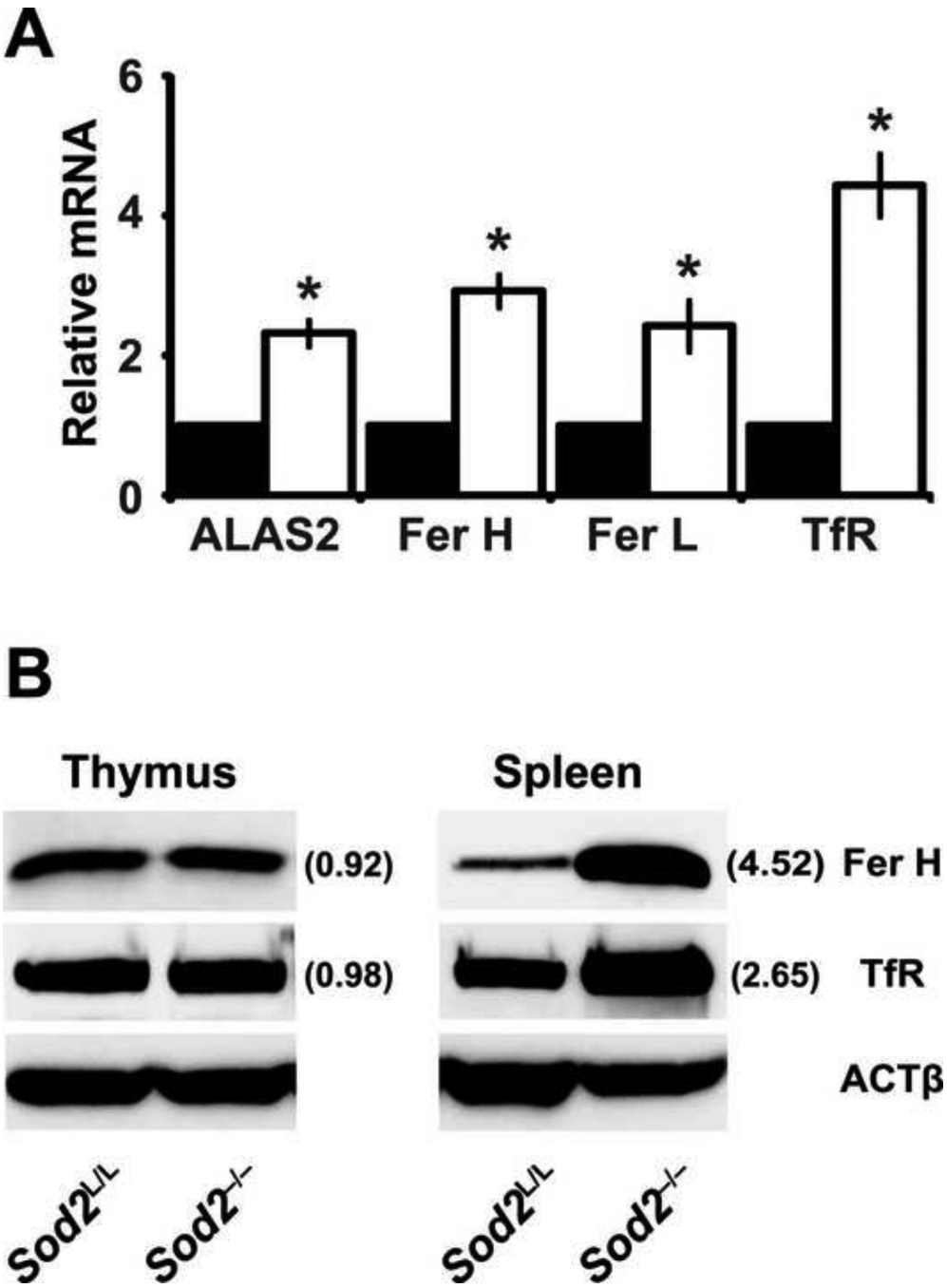

Figure 4. Iron responsive element-containing genes are up-regulated in *Sod2*$^{-/-}$ spleens

(A) Quantitative real-time RT-PCR analysis of genes containing iron regulatory elements (IRE). Data were normalized to 18s mRNA, then to respective *Sod2*$^{L/L}$ gene using the ΔΔCT method. Closed bars indicate *Sod2*$^{L/L}$, open bars indicate *Sod2*$^{-/-}$. Aminolevulinate synthase 2 (ALAS2); Ferritin heavy chain (Fer H); Ferritin light chain (Fer L); Transferrin receptor (TfR). Three mice of respective genotypes were analyzed per experiment; data are shown as mean and s.d. Where applicable, * = p<0.01 by Student's t-test versus *Sod2*$^{L/L}$. (B) Western blot analysis of iron regulatory element (IRE) containing proteins in hematopoietic tissues from 6-week old *Sod2*$^{L/L}$ or *Sod2*$^{-/-}$ mice. β-actin (ACTβ) shown as loading control. Quantification normalized to ACTβ, then to *Sod2*$^{L/L}$ using ImageJ software.

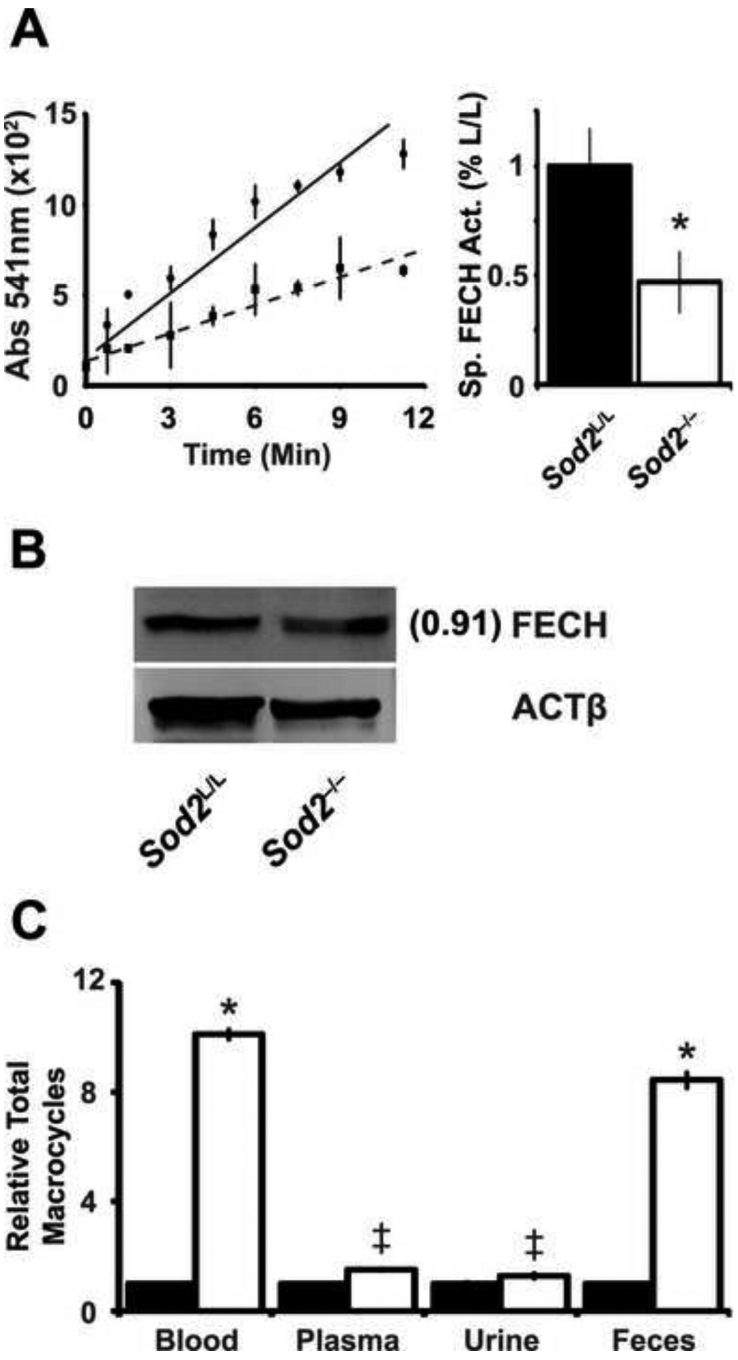

Figure. 5. Ferrochelatase activity is decreased by increased mitochondrial superoxide

(A) Ferrochelatase (FECH) activity assay performed on bone marrow extracted from 6-week old animals. Left, data displayed as absorbance of zinc-incorporated porphyrin over time. Solid line indicates *Sod2*$^{L/L}$, dotted line indicates *Sod2*$^{-/-}$. Right, quantification of FECH activity. Specific activity calculated based on relative FECH protein levels (panel B). Three mice of respective genotypes were analyzed per experiment; data are shown as mean and s.d. Where applicable, * = $p<0.01$ or ‡ = $p<0.05$ by Student's t-test versus *Sod2*$^{L/L}$. (B) Western blot analysis for ferrochelatase (FECH) protein in bone marrow from 6-week old *Sod2*$^{L/L}$ or *Sod2*$^{-/-}$ mice. β-actin (ACTβ) shown as loading control. Quantification normalized to ACTβ, then to *Sod2*$^{L/L}$ using ImageJ software. (C) Spectrophotometric assay

of iron-free macrocycles in various tissues in 6-week old *Sod2*$^{L/L}$ or *Sod2*$^{-/-}$ mice. Closed bars indicate *Sod2*$^{L/L}$, open bars indicate *Sod2*$^{-/-}$. Data normalized to respective *Sod2*$^{L/L}$ tissue.

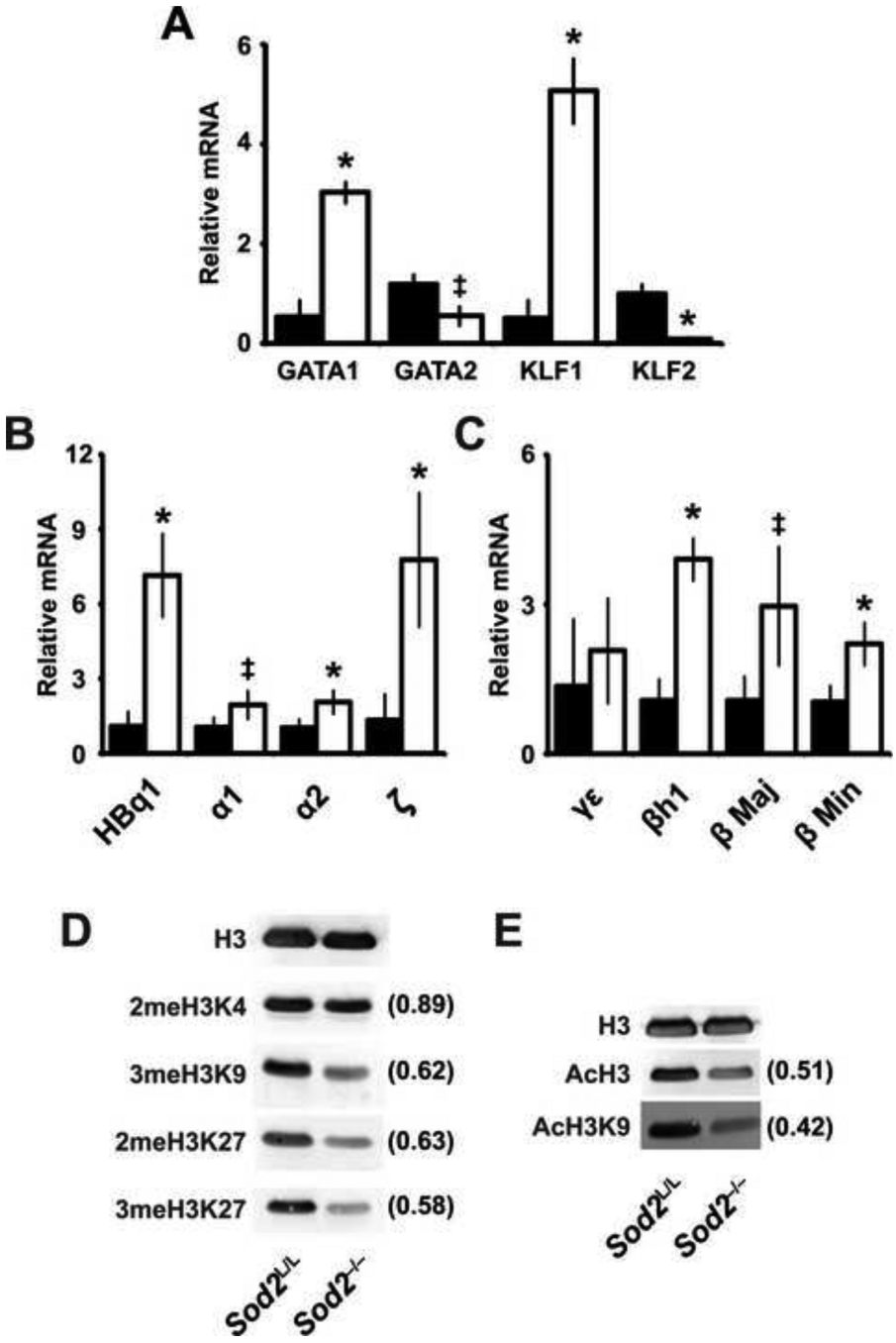

Figure. 6. Abnormal gene expression in spleens of *Sod2*$^{-/-}$ animals is associated with alterations in global histone acetylation and disruption of epigenetic control

(A) Quantitative real-time RT-PCR analysis of erythropoietic transcription factors from RNA extracted from spleens in 6-week *Sod2*$^{L/L}$ and *Sod2*$^{-/-}$ animals. Data were normalized to 18s mRNA, then to respective *Sod2*$^{L/L}$ gene using the ΔΔCT method. Closed bars indicate *Sod2*$^{L/L}$, open bars indicate *Sod2*$^{-/-}$. GATA-binding factor 1 (GATA1); GATA-binding factor 2 (GATA2); Kruppel-like factor 1 (KLF1); Kruppel-like factor 2 (KLF2). (B) Quantitative real-time RT-PCR analysis of alpha globins from RNA extracted from spleens in 6-week *Sod2*$^{L/L}$ and *Sod2*$^{-/-}$ animals. Data were normalized to 18s mRNA, then to respective *Sod2*$^{L/L}$ gene using the ΔΔCT method. Closed bars indicate *Sod2*$^{L/L}$, open bars

indicate *Sod2*$^{-/-}$. Theta (HBq1); alpha 1 (α1); alpha 2 (α2); zeta (ζ). (C) Quantitative real-time RT-PCR analysis of beta globins from RNA extracted from spleens in 6-week *Sod2*$^{L/L}$ and *Sod2*$^{-/-}$ animals. Data were normalized to 18s mRNA, then to respective *Sod2*$^{L/L}$ gene using the ΔΔCT method. Closed bars indicate *Sod2*$^{L/L}$, open bars indicate *Sod2*$^{-/-}$. Gamma-epsilon (γε); Beta-like (βh1); Beta major (β Maj); Beta minor (β Min). (D) & (E) Western blot analysis for various histone modifications in spleens from 6-week old *Sod2*$^{L/L}$ or *Sod2*$^{-/-}$ mice. Total H3 shown as loading control. Quantification normalized to total H3, then to respective *Sod2*$^{L/L}$ tissue using ImageJ software. Three mice of respective genotypes were analyzed per experiment; data are shown as mean and s.d. Where applicable, * = $p<0.01$ or ‡ = $p<0.05$ by Student's t-test versus *Sod2*$^{L/L}$.

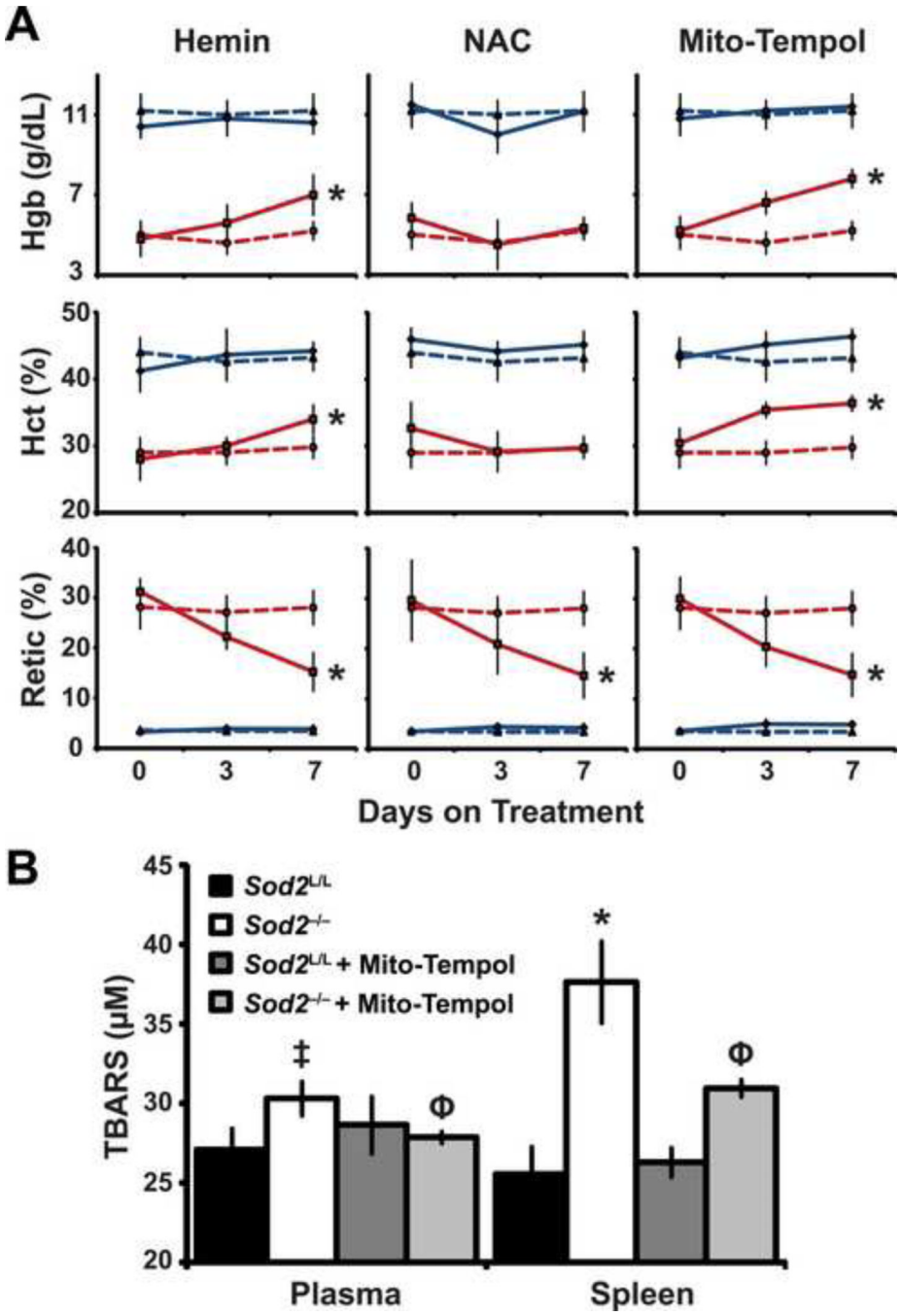

Figure. 7. Anti-oxidant therapy or hemin partially rescued the observed phenotype

(A) Mice were treated with respective drug for 7 days. Complete blood count (CBC) analysis performed on days 0, 3, and 7. Dotted blue line indicates *Sod2*$^{L/L}$ vehicle treated, Solid blue line indicates *Sod2*$^{L/L}$ drug treated, Dotted red line indicates *Sod2*$^{-/-}$ vehicle treated, solid red line indicates *Sod2*$^{-/-}$ drug treated. Hemoglobin (Hgb); Hematocrit (Hct); Reticulocytes (Retic). (B) Thiobarbituric acid reactive substances (TBARS) assay on total blood plasma and total spleen isolates with and without Mito-Tempol administration. Six mice of respective genotypes were analyzed per experiment; data are shown as mean and s.d. Where applicable, * = $p<0.01$ or ‡ = $p<0.05$ by Student's t-test versus *Sod2*$^{L/L}$; Φ = $p<0.01$ by Student's t-test versus *Sod2*$^{-/-}$.